Fish and Shellfish Immunology 78 (2018) 299–309

Contents lists available at ScienceDirect

Fish and Shellfish Immunology

journal homepage: www.elsevier.com/locate/fsi

Full length article

Molecular characterization of glutaminyl-peptide cyclotransferase(QPCT)in *Scylla paramamosain* and its role in *Vibrio alginolyticus* and white spot syndrome virus (WSSV) infection

Ziyan Wang, Baozhen Sun, Fei Zhu*

College of Animal Science and Technology, Zhejiang Agriculture and Forestry University, Hangzhou 311300, China

ARTICLE INFO

Keywords:
Scylla paramamosain
Glutaminyl-peptide cyclotransferase
Immune
White spot syndrome virus
Vibrio alginolyticus

ABSTRACT

Glutaminyl-peptide cyclotransferase (QPCT) catalyzes the posttranslational modification of an N-terminal glutamate of proteins to pyroglutamate. This renders the protein more resistant to protease degradation, more susceptible to hydrophobic interactions, aggregation, and neurotoxic. In this study, we evaluated the influence of QPCT in the crab *Scylla paramamosain* infected with white spot syndrome virus (WSSV) or with *Vibrio alginolyticus*. A cDNA clone, encompassing the entire 2445 bp of the *S. paramamosain* QPCT gene, containing a 1113 bp open reading frame (ORF) encoding a 370 amino acid protein was cloned from *S. paramamosain*. Real-time PCR indicated that *QPCT* was primarily expressed in the digestive tract of *S. paramamosain*, was up-regulated in hemocytes after infection with *V. alginolyticus,* and down-regulated in hemocytes after infection with WSSV. Knockdown of *QPCT* expression by double-stranded RNA (QPCT-dsRNA) resulted in down-regulation of prophenoloxidase (proPO) and crustin antimicrobial peptide, whereas myosin-II-essential-light-chain-like-protein was significantly up-regulated in hemocytes at 24 h post QPCT-dsRNA treatment. WSSV challenge in crabs treated with QPCT-dsRNA resulted in a reduction in viral burden and in the apoptotic rate of crab hemocytes, while the phagocytic activity of crab hemocytes and overall mortality rate were increased. This suggests that WSSV might take advantage of QPCT to benefit its replication. In contrast, *V. alginolyticus* infection in crabs treated with QPCT-dsRNA indicated that the apoptotic rate and phagocytic activity of hemocytes, and overall incidence of mortality, were increased compared to mock-treated animals, indicating that QPCT might be a resistance factor in bacterial infection. These results increase our understanding of the function of QPCT and its role in the innate immunity of *S. paramamosain*.

1. Introduction

The immune system in vertebrates consists of an innate and an adaptive response [1]; however, all crustaceans, including *S. paramamosain,* rely solely on innate immunity to provide a highly efficient defense against infection [2,3]. They have the nonspecific immune to recognize and eliminate the invasion of foreign body, to keep the balance of the body both inside and outside osmotic pressure, aiming to protect the body. As two of the most serious diseases in crabs, vibriosis and white spot syndrome virus (WSSV) have caused irreversible damage to the crab culture industry worldwide [4]. *V. alginolyticus* is one kind of important pathogens in oceans. Just like other pathogens, many sorts of virulence factors that base on virulence gene mainly result in its pathogenicity [5]. *S. paramamosain* was a natural host of WSSV, which could be infected with WSSV by consuming diseased shrimp and become a medium of WSSV in a polyculture system of shrimp and crab [6]. At present there are no efficient measures to control either of these diseases.

The QPCT gene encodes glutaminyl cyclase (QC), an enzyme which performs the posttranslational modification of protein by converting an N-terminal glutamate to pyroglutamate. This renders the protein more resistant to protease degradation, more hydrophobic, more prone to aggregation and neurotoxic. In the mouse, the QPCT transcript is located on chromosome 17 (chr17:79451246–79489583) and encodes glutaminylcyclase, a Zn^{2+}-dependent acyltransferase with a mixed α-helix and β-sheet structure. QC has been isolated from animals, plants, and bacteria [7]. Recently, it has been found that QPCT has a close relationship with some cancers, such as melanoma, papillary thyroid carcinoma, and renal cell carcinoma [8]. The function and mechanism of glutaminyl peptide cyclase in human osteoporosis and in schizophrenia has been extensively studied, but the function and role of glutathione-peptidyl-transferase has not been studied in crustaceans.

* Corresponding author.
E-mail address: zhufei@zju.edu.cn (F. Zhu).

https://doi.org/10.1016/j.fsi.2018.04.059
Received 6 February 2018; Received in revised form 21 April 2018; Accepted 26 April 2018
Available online 27 April 2018

Herein, we report the influence of QPCT in the innate immune system of *S. paramamosain* upon viral and bacterial infection.

2. Methods and materials

2.1. Crabs and tissue preparation

Healthy adult *S. paramamosain* (approximately 100 g) were obtained from a seafood market of Hangzhou. All animal experiments were reviewed and approved by the Institutional Animal Care and Use Committee of Zhejiang A & F University (Hangzhou, China). The muscle, hepatopancreas, gills, sex organs, and hemolymph were collected from control or from QPCT-dsRNA treated crabs. Samples were immediately processed for RNA extraction. WSSV (GenBank accession no. AF 332093.3) was purified and used in infection experiments, as described previously [9]. *V. alginolyticus* was cultured and used to infect crabs according to a previous report [10].

2.2. Rapid amplification of cDNA ends (RACE)

Total RNA was extracted from hemocytes of the *S. paramamosain* using PureLink™ RNA Mini Kit (Ambion, USA), following the protocol of the manufacturer. The concentration and quality of total RNA were determined by the Nanodrop Trace Spectrophotometer and 1% agarose gel electrophoresis detection, respectively. The RACE technique was utilized to clone the full-length cDNA sequence of the gene, based on the known middle fragment using SMARTer® RACE 5′/3′Kit, following the protocol of the manufacturer. The synthesized cDNA were kept at -20 °C, used for the 3′/5′ -RACE PCR with 3′ gene-specific primer (3GSP1, 3NGSP1) or 5′ GSP (5GSP2, 5NGSP2), designed on the basis of middle sequence (the primers sequences are shown in Table 1). The PCR products were purified using MiniBEST DNA Fragment Purification Kit Ver.3.0 (Takara, Japan), following the manufacturer's instruction. Amplified cDNA fragments were transferred into the pMD19-T vector (Takara, Japan). Recombinant bacteria were identified by blue/white screening and confirmed by PCR and sent to sequencing company (Sangon, China). Nucleotide sequences of the cloned cDNA were sequenced by double pass. All primers used in this experiment were designed using Primer Premier 5.0.

2.3. Nucleotide sequence and bioinformatics analyses

The nucleotide sequence similarities were examined by BLAST software (http://www.ncbi.nlm.nih.gov/BLAST/). The 5′and 3′sequences from RACEs were assembled with the partial cDNA sequences corresponding to each fragmental sequence by DNAMAN 5.0. The protein prediction was performed using the open reading frame (ORF) Finder tool. Multiple sequence alignment was created by using the DNAMAN 5.0. And the phylogenetic trees based on the amino acid sequences were performed by the neighbor-joining method using Molecular Evolutionary Genetics Analysis, MEGA 7.1.

2.4. The quantitative real-time PCR

Relative QPCT mRNA expression levels in various adult tissues were measured by qRT-PCR using a SYBR II® Premix Ex Taq (Tli Rnase Plus) (TaKaRa, Japan). Total RNA was isolated from various tissues of healthy adult crabs and hemocytes of crabs challenged by intramuscular injection of 0.2 mL of viral or bacterial suspension including WSSV (10^5 copies/mL) or *V. alginolyticus* (10^5 colony-forming units [CFU]/mL), respectively, for different times, using the EASY spin tissue/cell RNA extraction kit (Aidlab, China) according to the manufacturer's instructions. Experiments were performed in triplicate and at least three crabs were analyzed for each tissue type. The cDNA synthesis was carried out using 200 μg of total RNA with the ReverTra Ace qPCR RT Master Mix with gDNA Remover (Code: FSQ-301; Toyobo, Japan). The synthetic cDNA was kept at −20 °C. RT-qPCR was carried out in Bio-Rad Two Color Real-Time PCR Detection System and the data were calculated according to the $2^{-\Delta\Delta CT}$ comparative CT method by Office Excel, with GAPDH amplification as the internal control [11]. The design and synthesis of the RT-qPCR primers were entrusted to Generay (Shanghai, China), based on the open reading frame (ORF). Table 1 lists the primers that were designed and synthesized by Generay.

Table 1
Primer sequences and purpose.

Name	Nucleotide Sequence (5′ to 3′)	purpose
3′ race GSP1	TGGTGTCCTACGAACGGCGTCTGAG	first primer for 3′ RACE
3′ race NGSP1	CCGATTATCTCCACTTGGTCCT	second primer for 3′ RACE
5′ race GSP2	CCACCACTCGAGGCACCAGGATG	first primer for 5′ RACE
5′ race NGSP2	CCACACACATCCACCGAGGAACCAT	third primer for 5′ RACE
QPCT-realtime-F	TAGAGTGAGGGGTTGGTG	for QPCT expression
QPCT-realtime-R	GAGTGAAATGGAGAGATGGA	for QPCT expression
GAPDH-realtime-F	ACCTCACCAACTCCAACAC	for GAPDH expression
GAPDH-realtime-R	CATTCACAGCCACAACCT	for GAPDH expression
QPCT dsRNA F	*CCC*AAGCTTAGGGACACA CCAGAGTGAGGCAG	for QPCT RNAi
QPCT dsRNA R	*ACGC*GTCGACTTGTTGGTG GGATAAGCCCGAGC	for QPCT RNAi
JAK -F	ATTGCTGAGGGGATGGATT	for JAK expression
JAK -R	GCCCATCACATTCCCAAA	for JAK expression
STAT -F	GACTTCACTAACTTCAGCCTCG	for STAT expression
STAT -R	GAGCTGAGTCTGTCTTAATGTTATCC	for STAT expression
C-type-lectin-F	ACTGAGGGGAAAGTAGCC	for C-type-lectin expression
C-type-lectin-R	TGCCCGTGTTTATTCATC	for C-type-lectin expression
crustin-F	TCAGAGCACCCTGGTAAATGT	for crustin antimicrobial peptide expression
crustin-R	GGCAGAACTGCGAAAGAAAG	for crustin antimicrobial peptide expression
TLR-F	TGTTGCCAGAGCAGAAGGT	for toll-like receptor expression
TLR-R	TTCCGTGAATGAACGAAGG	for toll-like receptor expression
proPO-F	ATGAAAGAGGAGTGGAGATG	for prophenoloxidase expression
proPO-R	GTGATGGATGAGGAGGTG	for prophenoloxidase expression
myosin-F	GCCGAGATAAGTGTAGAGGAA	for myosin-II-essential-light-chain-like-protein expression
myosin-R	AGTGGGGTTCTGTCCAAG	for myosin-II-essential-light-chain-like-protein expression

2.5. Prokaryotic expression and purification of QPCT-dsRNA

The primers (shown in Table 1) with specific restriction sites (*Hind* III in the forward primer and *Sal* I in the reverse primer) were designed from the cloned nucleotide sequence. PCR product digested with *Hind* III/*Sal* I was subcloned into LIMTUS 38i Vector (NEB, MA, USA) digested with the same enzymes to gain plasmid L38-QPCT. The constructed L38-QPCT was verified by restriction enzyme digestion and DNA sequencing. The recombinant plasmid L38-QPCT was transformed into HT115 (DE3) cells. Single colonies of the above engineering bacteria were separately inoculated to 5 mL of LB medium containing Amp (ampicillin) (100 μg/mL), cultured at 37 °C with shaking at 200 r/min for 12-16 h, and then inoculated to LB medium containing Amp by aproportion of 1%, cultured at 37 °C with shaking at 200 r/min for 2-3 h (OD600 ≈ 0.6), and added with IPTG (isopropyl-β-*d*-thiogalactoside) (with a final concentration of 0.8 mM/L) to induce the expression for 4 h. After purifying with mir Vana miRNA™ Isolation Kit (Ambion, USA), the xx-dsRNAs were annealed and precipitated with 5 M sodiumacetate and anhydrous alcohol. The EGFP-dsRNA was used as the control. Enhanced GFP (EGFP) belongs to one of the GFP. The green fluorescent protein (GFP) is a protein composed of 238 amino acid residues (26.9 kDa) that exhibits bright green fluorescence when exposed to light in the blue to ultraviolet range. GFP makes for an excellent tool in many forms of biology due to its ability to form internal chromophore without requiring any accessory cofactors, gene products, or enzymes/substrates other than molecular oxygen.

2.6. Knock down of QPCT by RNAi and challenge experiments

Total RNA was purified using an EASY spin tissue/cell RNA extraction kit (Aidlab, China), following the manufacturer's instructions. QPCT-dsRNAs (75 μg/crab) was immediately injected intramuscularly into the fourth pereopodcoxa of each crab, and QPCT mRNA expression levels were detected by qRT-PCR following WSSV and *V. alginolyticus* challenge.

2.7. Quantitative analysis of WSSV

TaqMan real-time PCR was performed by using a Perfect Real Time premix (Takara, Japan) containing a high-performance Taq antibody, Takara Ex Taq HS, for hot start real-time PCR. Primers were designed using Primer 5.0 software and the TaqMan probe with the WSSV whole sequence. Primers WSSV-RT1 (5′-TTGGTTTCATGCCCGAGATT-3′) and WSSV-RT2 (5′-CCTTGGTCAGCCCCTTGA-3′) produced a fragment of 154 bp after amplification. The TaqMan probe was synthesized and labeled with the fluorescent dyes 5-carboxyfluorescein (FAM) (5′-FAM-TGCTGCCGTCTCCAA-TAMRA-3′). PCR amplification was performed for 4 min at 50 °C, followed by 45 cycles of 45 s at 95 °C, 45 s at 52 °C and 45 s at 72 °C. Thermal cycling was performed on an iCycle IQ5 real-time PCR detection system (Bio-RAD, USA).

2.8. Kaplan–Meier survival analysis

For the pathogen challenge, healthy crab were randomly distributed into six groups (n = 9 per group, three repeat). The control group received injections of PBS alone, the QPCT-dsRNA group received injections of QPCT-dsRNA alone, the WSSV group received injections of WSSV in PBS, and the QPCT-dsRNA + WSSV group received injections of QPCT-dsRNA and WSSV, the *V. alginolyticus* group received injections of *V. alginolyticus* in PBS, and the QPCT-dsRNA + *V. alginolyticus* group received injections of QPCT-dsRNA and *V. alginolyticus*. Each group of crabs was cultivated under the same condition. After every 12 h, the number of live and dead crab was counted. The survival data was arranged and analyzed in Microsoft GraphPad 5.0.

2.9. Phagocyte rate counting by flow cytometry

Experimental and control groups were injected with dsRNA and PBS, respectively. In brief, 2.5 mL syringe was used to collect the hemolymph from the last walking legs of crabs which sterilized with 70% alcohol with half volume of pre-cooled anticoagulant solution (20 mM EDTA, PH 6.4), and the mixture was centrifuged at 2000 rpm at 4 °C for 10min to collect hemolymph cells. The subsequent experiment was performed as described previously [12,13].

2.10. Apoptosis of crab hemocytes

The hemolymph was mixed with 20 mM EDTA at a ratio of 1:1, and the mixture was centrifuged at 2000 rpm at 4 °C for 10 min to collect hemolymph cells. The hemolymph cells were then suspended in highly alkaline PBS, counted and adjusted to a density of 3-5 × 10^6 cells/mL with PBS. The cells were stained using a BD Phrmingen™ FITC Annexin V Apoptosis Kit, and assessed by flow cytometry. The cell numbers on quadrant 4, with low PI and high annexin V staining, were considered as apoptotic. The data were presented as means ± standard deviation (SD) derived from at least three independent experiments.

2.11. Determination of immune parameters after RNAi

The immune parameters determined included total hemocytes numbers (THC), PO and SOD activities. THC was determined as described previously [14]. To determine PO and SOD activities, 500 μL hemolymph was withdrawn into a 1 mL syringe containing 500 μL 20 mM EDTA solution from each individual crab. PO activity was quantified in the hemolymph mixture based on the formation of dopa chrome from the substrate L-3, 4-dihydroxyphenylalanine (L-DOPA), as described previously [15]. SOD activity was quantified in hemocytes isolated from 300 μL of the hemolymph mixture, according to the improved method described by Beauchamp and Fridovich [16]. Data were presented as a percentage of the normal control.

2.12. Statistical analysis

Quantitative data were expressed as mean ± standard deviation (SD). Data from three independent experiments were analyzed by one-way analysis of variance to calculate the means and standard deviations of the triplicate assays. Statistical differences were estimated using one-way ANOVA followed by least-significant differences (LSD) and Duncan's multiple range test. All statistics were measured using SPSS software version 19 (IBM, USA). Aprobability level of 0.01 was used to indicate statistical significance ($P < 0.01$).

3. Results

3.1. Characterization of the S. paramamosain QPCT transcript

The full-length QPCT cDNA sequence we obtained was 2445 base pairs (bp) in length and contained a 1113 bp open reading frame (ORF) encoding a 370 amino acid protein. The 3′ untranslated region (UTRs) was 1,333bp in length. The nucleotide and deduced amino acid sequence of the full-length cDNA are shown in Fig. 1.

3.2. Sequence homology and phylogenetic analysis

The predicted amino acid sequences of *S. paramamosain* QPCT were compared with the sequence of QPCT from vertebrates and invertebrates. The results revealed *S. paramamosain* QPCT has a similarity of 48% with that of *Bombyx mori*, 38% compared to *Danio rerio*, 43% to *Homo sapiens*, 43% to *Mus musculus*, 43% to *Bactrocera dorsalis*, 40% to *Bombus impatiens,* and 47% to *Xenopus tropicalis* (Fig. 2).

A condensed phylogenetic tree, based on the deduced amino acid

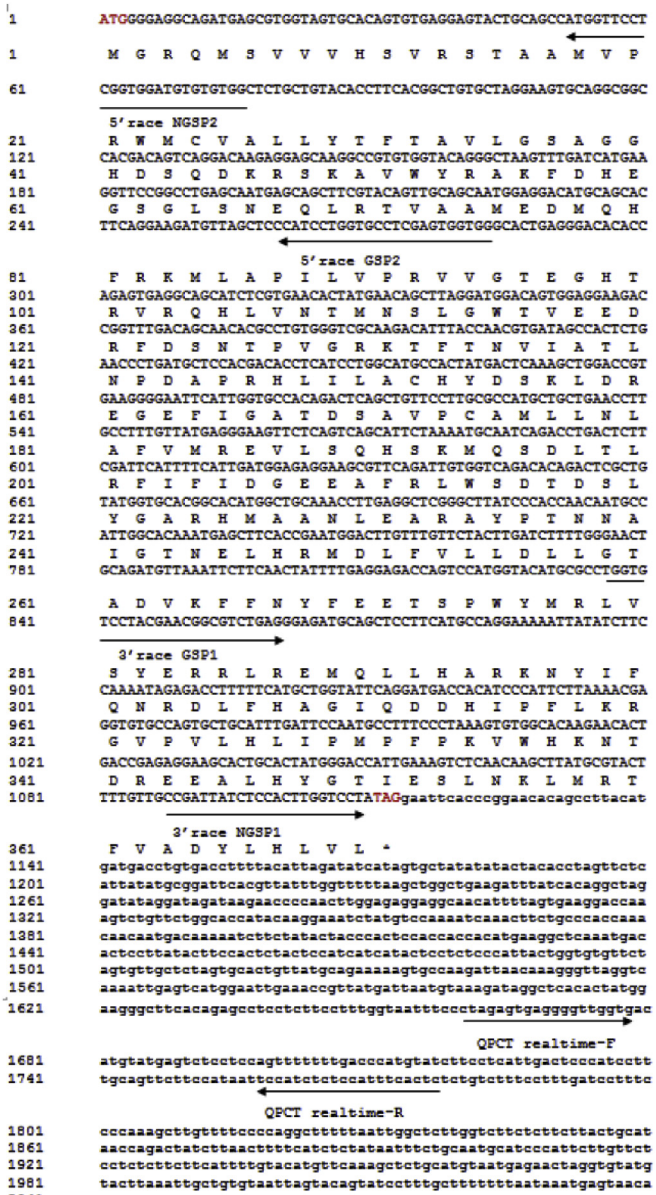

Fig. 1. Nucleotide and deduced amino acid sequence of QPCT. The nucleotide sequence is displayed in the 5′-3′ direction. The deduced amino acid sequence is shown as single letter amino acid code. The 3′ UTR and 5′ UTR regions are indicated by lower case letters. Codons are numbered from the initiating methionine (ATG) codon, with an asterisk denoting the termination codon (TAG). RACE and real-time qPCR primers are marked with arrows.

sequences of QPCT from a broad range of animals, was constructed by the neighbor-joining method (Fig. 3). Among known species, *S. paramamosain* QPCT was most similar to that of *Trichinella spiralis*.

3.3. Tissue expression profiles of QPCT mRNA

Expression profiling of the QPCT gene in different tissues of *S. paramamosain* was examined by quantitative real-time polymerase chain reaction (qRT-PCR) (Fig. 4). QPCT was significantly more highly expressed in the digestive tract as compared to other tissues, and showed the lowest expression in muscle. Expression levels of QPCT in

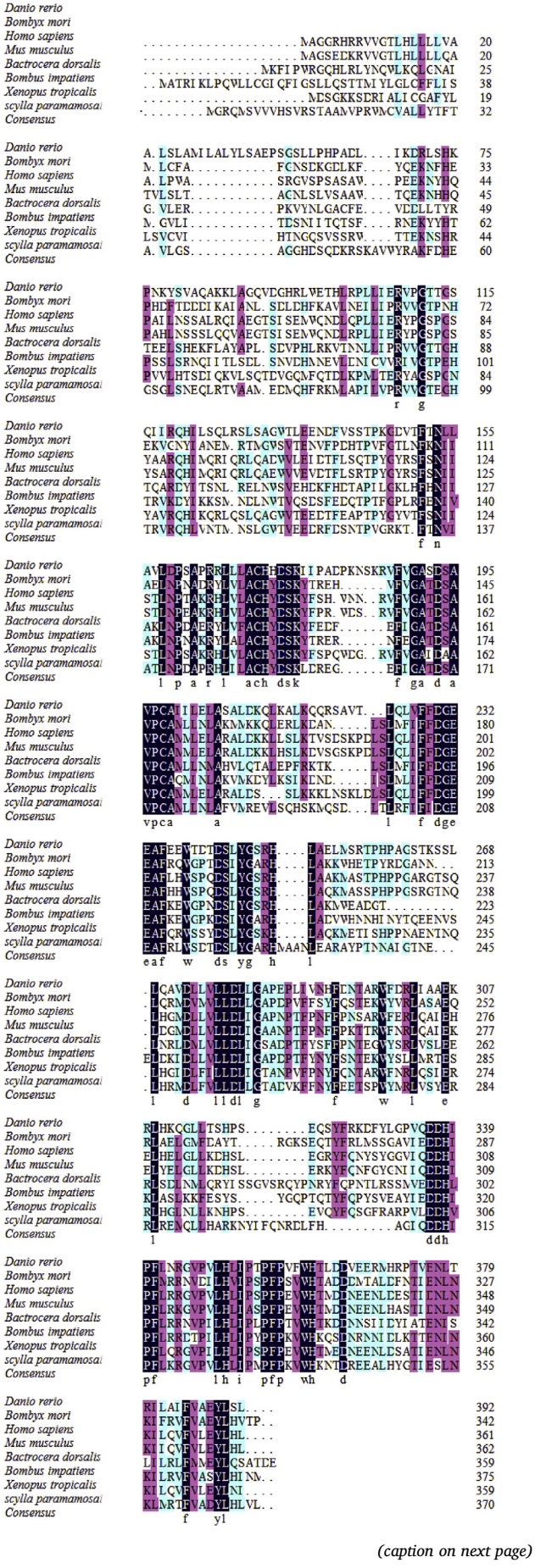

(caption on next page)

Fig. 2. Multiple alignment of the amino acid sequence of *S. paramamosain* QPCT with *Danio rerio* (NP_001038418.1), *Bombyx mori* (XP_012546494.1), *Homo sapiens* (CAA50438.1), *Mus musculus* (AAI51030.1), *Bactrocera dorsalis* (JAC46018.1), *Bombus impatiens* (XP_003487058.1), and *Xenopus tropicalis* (NP_001017245.1). Twelve conserved cysteines (C1 –C12) are shaded and boxed.

the intestines were 3.66, 2.09, 1142.74, 34.87, 5.76, and 3.27-fold greater than that in the hemolymph, gills, muscle, heart, hepatopancreas, and gonad, respectively. The expression of QPCT in the intestine was significantly higher ($P < 0.01$) than in any other tissue evaluated. The cause of this phenomenon maybe that intestinal has diverse microorganisms in mud crab, microorganisms produce and secrete a variety of enzymes, maintaining itself the microbial metabolism and helping absorb conversion and absorption of food and medicine [17,18].

3.4. The time course of QPCT expression after infection with WSSV or V. alginolyticus

We investigated the expression of QPCT in crabs after infection with WSSV or with *V. alginolyticus*. We observed that QPCT expression changed after infection in a time-dependent manner. QPCT expression was significantly down-regulated ($P < 0.01$) between 12 and 48 h post infection in WSSV-infected crabs. The lowest expression level occurred at 24 h, after which QPCT mRNA gradually returned to pre-infection levels with full recovery 48 h after initiating infection (Fig. 5A). In contrast, expression of QPCT was significantly up-regulated ($P < 0.01$) at 12 and 48 h following infection with *V. alginolyticus*, but again gradually returned to pre-infection levels 48 h after initiation of infection

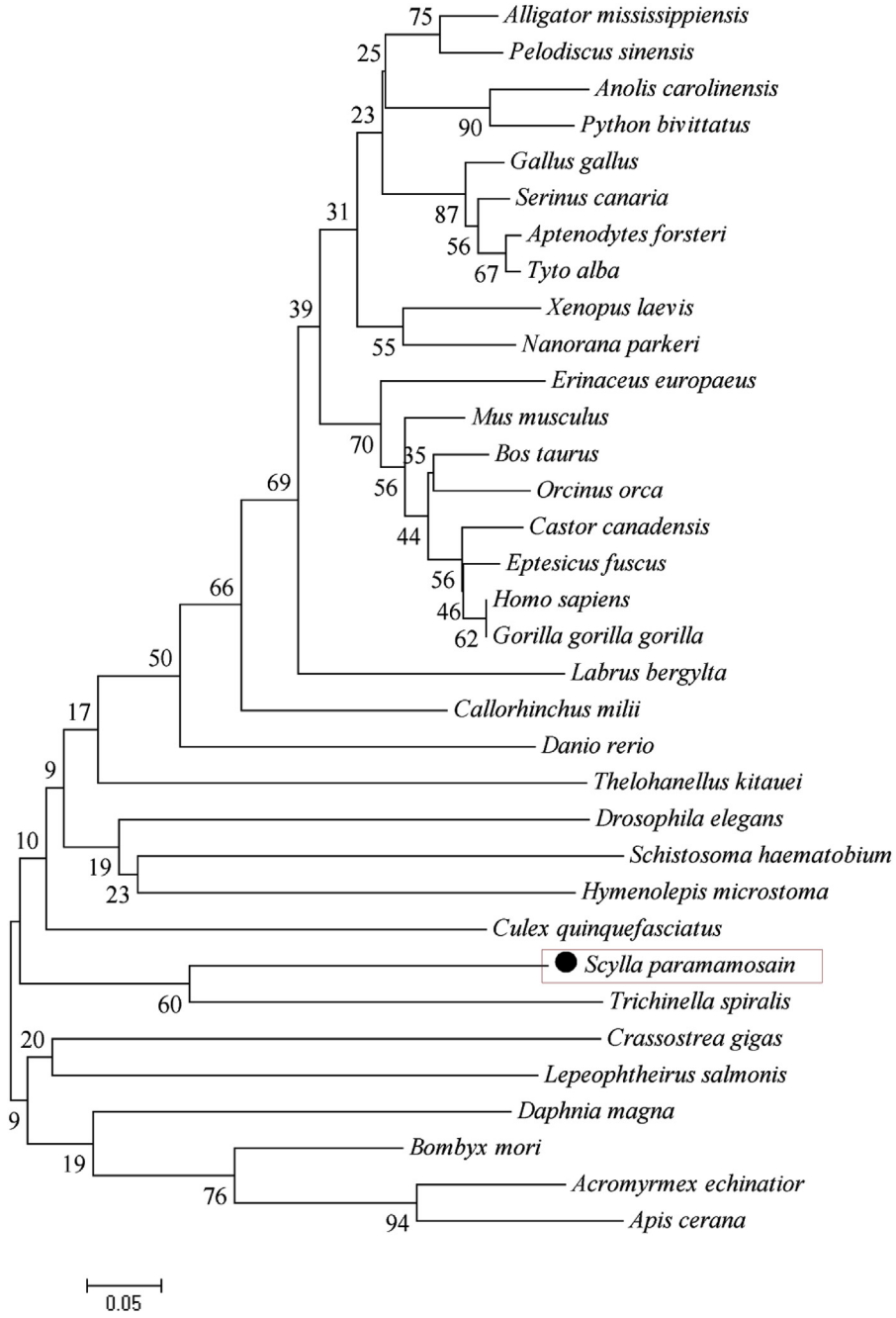

Fig. 3. The phylogenetic relationship of QPCT from different organisms based on amino acid sequence comparisons.

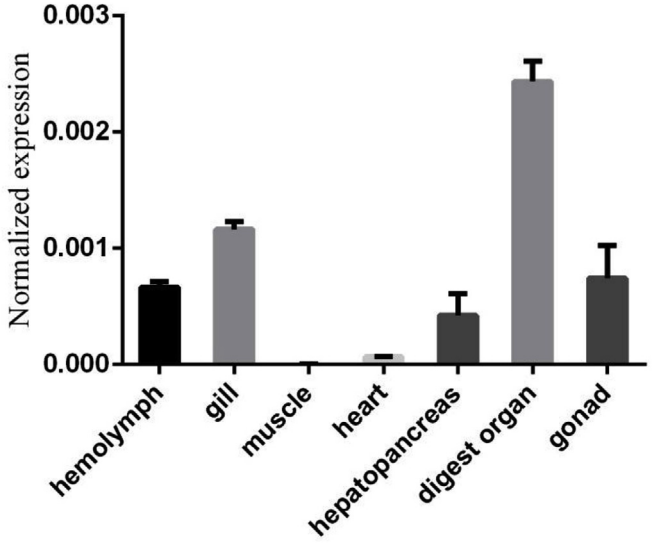

Fig. 4. Expression levels of QPCT in various tissues of *S. paramamosain* were determined by quantitative real-time PCR. The amount of QPCT mRNA was normalized to GAPDH transcript levels. Data are shown as the mean ± SD (standard deviation) from three individuals.

(Fig. 5B). These results suggested that QPCT may play an important role in the innate immunity of crabs infected with WSSV or with *V. alginolyticus*.

3.5. Effect of double-stranded RNA inhibition of QPCT expression on immune genes

We tested the effect of QPCT double-stranded RNA (QPCT-dsRNA) on the expression of QPCT using RT-PCR. QPCT mRNA expression in crab hemocytes was significantly reduced by QPCT-dsRNA ($P < 0.01$) (Fig. 6A), from 24 to 48 h after treatment (Fig. 6B). We next examined the relationship between QPCT expression levels and the expression of other immunity-related genes in the hemocytes of crabs. Among the seven immune genes evaluated, prophenoloxidase (proPO) and crustin antimicrobial peptide were significantly down-regulated ($P < 0.01$), while myosin-II-essential-light-chain-like-protein was significantly up-regulated ($P < 0.01$) following treatment with QPCT-dsRNA (Fig. 6C). The expression levels of all evaluated transcripts were not altered significantly in crabs treated with EGFP-dsRNA.

3.6. Determination of immune parameters

Phenoloxidase (PO) activity was significantly increased ($P < 0.01$) (Fig. 7A) at 24 and 48h in crabs treated with QPCT-dsRNA. There was no significant change in superoxide dismutase (SOD) activity (Fig. 7B). PO and SOD activities in EGFP-dsRNA-treated crabs were similar to those in animals receiving PBS. Together, these results indicated that QPCT had a stimulatory effect on the immune system of crabs.

3.7. The effect of reducing QPCT expression on survival and on the extent of WSSV infection

The number of WSSV virions increased with the duration of infection in all groups; however, WSSV levels were 10-fold lower in the QPCT-dsRNA-treated group compared with control animals (Fig. 8). At 48 h post infection, the concentration of WSSV reached 10^3 copies in the control group but under 10^3 copies in the experimental group. Thereafter, the numbers continued to increase to 10^5 and 10^4 copies per X, respectively, after which the level of WSSV infection plateaued. Compared with the control groups, crabs pretreated with QPCT-dsRNA had a lower number of virions, suggesting that a reduction in QPCT

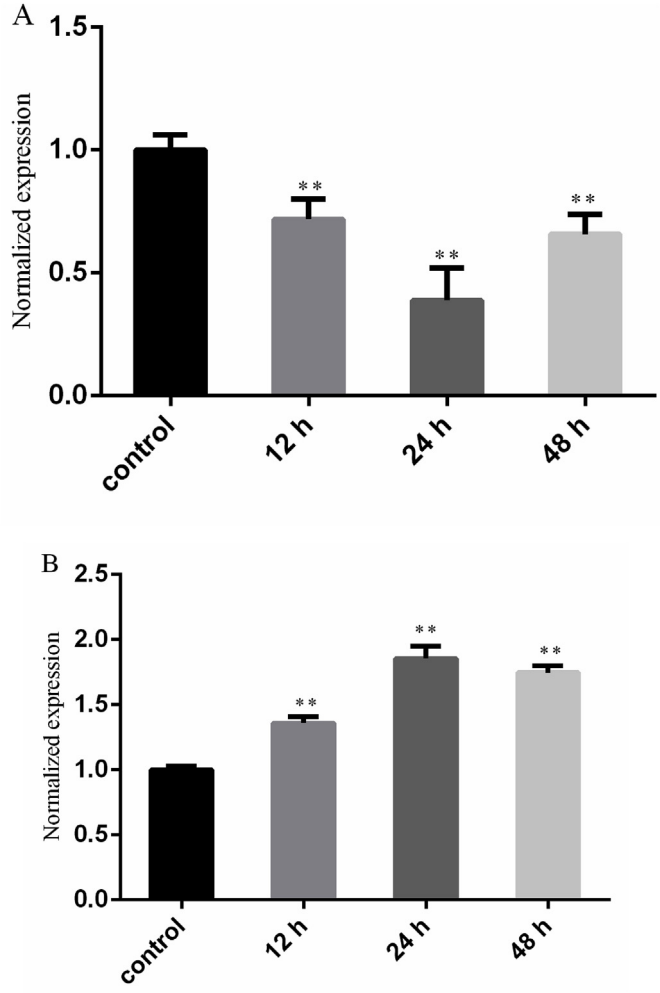

Fig. 5. Real-time RT-PCR analysis of QPCT expression in hemocytes of *S. paramamosain* infected with WSSV or *V. alginolyticus*. (A) Real-time RT-PCR analysis of QPCT expression in the hemocytes of *S. paramamosain* challenged with WSSV. (B) Real-time RT-PCR analysis of QPCT expression in the hemocytes of *S. paramamosain* challenged with *V. alginolyticus*. The level of QPCT mRNA was normalized to the GAPDH transcript level. Data are shown as the mean ± SD (standard deviation) of three animals. Double asterisks indicate a significant difference ($P < 0.01$) from QPCT levels prior to infection.

levels significantly ($P < 0.01$) inhibited the replication of WSSV.

We evaluated the effect of QPCT on the mortality of pathogen-challenged crabs by first treating them with QPCT-dsRNA and afterwards challenging them with *V. alginolyticus* or with WSSV. As shown in Fig. 9A, the QPCT-dsRNA-treated group showed higher mortality than the control group between 12 and 120 h, but thereafter, from 120–144 h post challenge, it had a lower mortality. The negative control group had a cumulative mortality of zero, demonstrating that crabs treated with QPCT-dsRNA showed no significant difference in mortality as compared to PBS-treated animals. This indicated that the ds-RNA was not toxic to crabs. In contrast, the cumulative mortality in crabs first treated with QPCT-dsRNA then infected with *V. alginolyticus* was significantly higher than when infected with *V. alginolyticus* ($P < 0.01$), starting from 240 h post infection (Fig. 9B). Overall, these results indicated that QPCT decreased the severity of WSSV infection, while, in contrast, a reduction in QPCT levels increased mortality following *V. alginolyticus* infection.

3.8. Influence of QPCT knockdown on total hemocyte count

The total hemocyte count (THC) was significantly increased

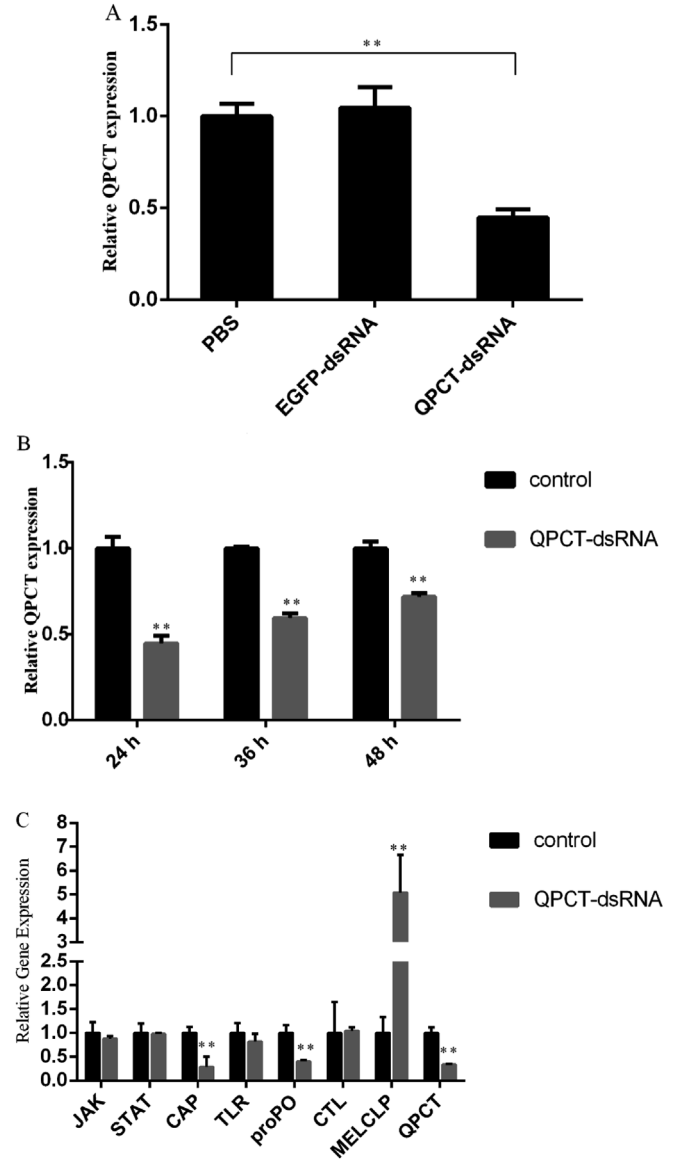

Fig. 6. Real-time RT-PCR analysis of the expression of QPCT and of selected innate immune genes. (A) Real-time PCR analysis of QPCT expression in hemocytes of *S. paramamosain* treated with QPCT dsRNA (QPCT-dsRNA) at 24 h post treatment. The amount of QPCT mRNA was normalized to the level of GAPDH mRNA. (B) Real-time RT-PCR analysis of QPCT expression in hemocytes of *S. paramamosain* treated with QPCT-dsRNA at different times post treatment. (C) Real-time RT-PCR analysis of seven immune genes (JAK, STAT, crustin antimicrobial peptide (CAP), toll-like receptor (TLR), prophenoloxidase (proPO), C-type-lectin (CTL), and myosin-II-essential-light-chain-like-protein (MELCLP) expression in the hemocytes of *S. paramamosain* treated with QPCT-dsRNA. The amount of QPCT mRNA was normalized to the level of GAPDH transcripts. Data are shown as mean ± SD (standard deviation) of three animals. Double asterisks indicate a significant difference ($P < 0.01$) between samples.

($P < 0.01$) at 24 and 48 h after WSSV infection, as compared with phosphate-buffered saline (PBS)-treated controls. Pretreatment with QPCT-dsRNA prior to challenge with WSSV resulted in a large decrease in THC (Fig. 10A). THC was significantly increased ($P < 0.01$) at 24 and 48h after infection with *V. alginolyticus*; pretreatment with QPCT-dsRNA had little effect on this increase at 24 and 48 h post-treatment (Fig. 10B). These results suggested that QPCT may positively regulate hemocyte proliferation in crabs.

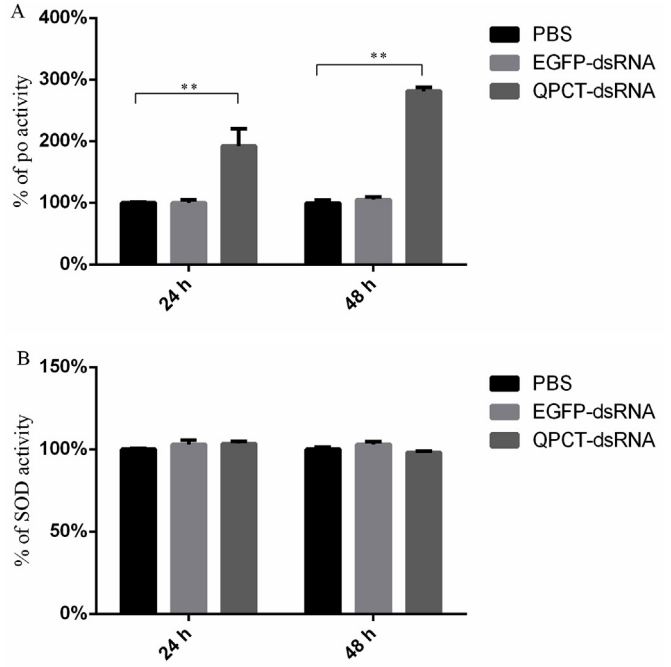

Fig. 7. PO and SOD activity of *S. paramamosain* hemocytes treated with QPCT-dsRNA. (A) PO activity of hemocytes from crabs treated with QPCT dsRNA, EGFP-dsRNA or with PBS. (B) SOD activity of hemocytes from crabs treated with QPCT dsRNA, EGFP-dsRNA or with PBS. Data are expressed as percentage of control. Double asterisks indicate a significant difference ($P < 0.01$) between the sample and the control.

3.9. Effect of reduced expression of QPCT on phagocytosis

Phagocytosis, as estimated by flow cytometry, was significantly increased in the group of crabs first treated with QPCT-dsRNA, then infected with WSSV, as compared to crabs infected with WSSV (55.8% vs. 31.4%), (Fig. 11D). Phagocytosis was also significantly increased in the group of crabs first treated with QPCT-dsRNA, then infected with *V. alginolyticus,* compared to crabs infected with *V. alginolyticus* (13.4% vs. 5.8%) (Fig. 11H). The extent of phagocytosis was similar in EGFP-dsRNA-treated crabs and in controls. These results suggested that a reduction in QPCT may reduce phagocytotic activity.

3.10. Effect of reduced expression of QPCT on apoptosis

We investigated the role of QPCT in apoptosis of crab hemocytes using flow cytometry. The rate of apoptosis was significantly lower in crabs pretreated with QPCT-dsRNA prior to challenge with WSSV compared with crabs infected with WSSV (9.7% vs.17.9%). In contrast, the apoptosis rate was significantly increased in the group of crabs first treated with QPCT-dsRNA, then infected with *V. alginolyticus,* compared to crabs infected with *V. alginolyticus* (Fig. 12). These results suggested that QPCT had an inhibitory effect on hemocyte apoptosis in crabs infected with *V. alginolyticus*, and a stimulatory effect on hemocyte apoptosis in crabs infected with WSSV.

4. Discussion

QPCT encodes glutaminyl-peptide cyclotransferase, an enzyme which performs a posttranslational modification of protein by converting an N-terminal glutamate to pyroglutamate. This renders the modified protein more resistant to protease degradation, more hydrophobic, prone to aggregation and neurotoxic. The expression level of QPCT is highest in the brain and consequently, understanding how QPCT expression is regulated is instrumental to a greater understanding

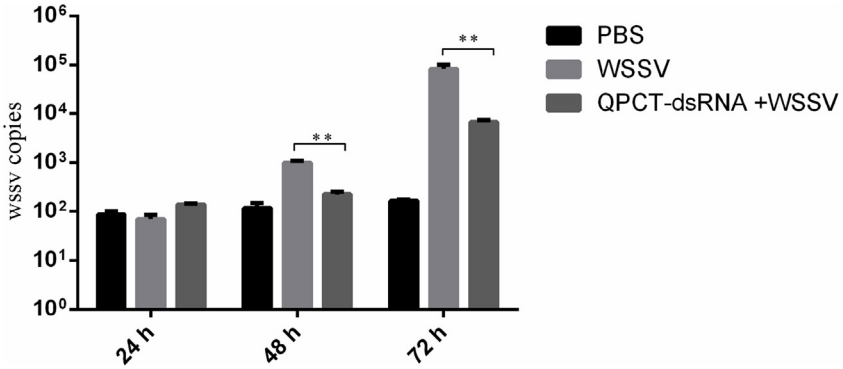

Fig. 8. Detection of WSSV viral load in hemocytes at different times following infection. Double asterisks indicate a significant difference ($P < 0.01$) between the sample and the control.

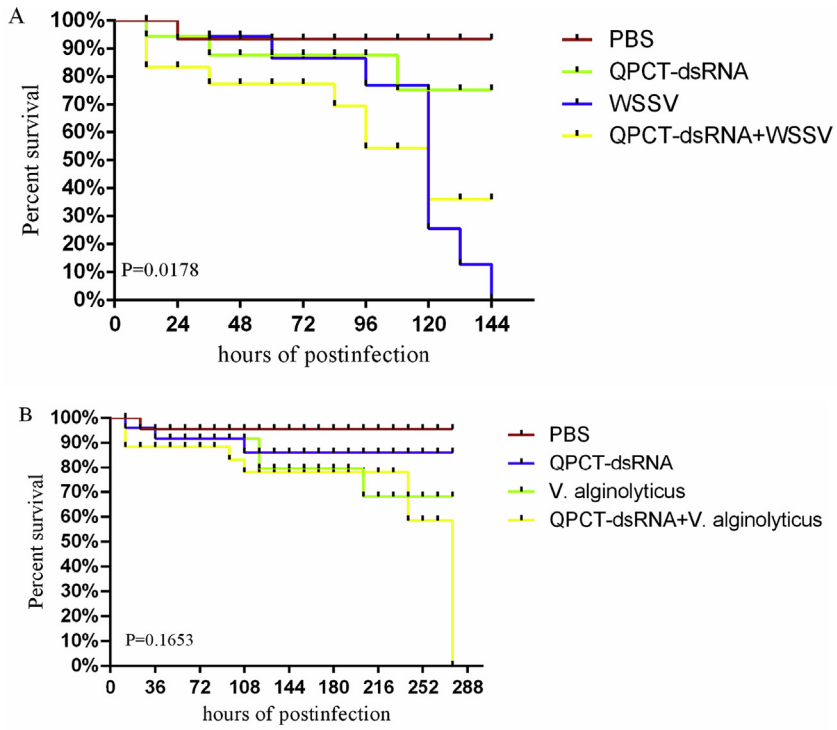

Fig. 9. Survival analysis of infected crabs pretreated with QPCT-dsRNA. (A) Kaplan-Meier survival analysis of WSSV infected crabs pretreated with QPCT dsRNA (QPCT-dsRNA). (B) Kaplan-Meier survival analysis of *V. alginolyticus* infected crabs pretreated with QPCT-dsRNA. The treatment regime applied to each group is indicated; n = 9.

of learning and memory. Furthermore, it has been reported that QPCT has a close relationship with some cancers, such as melanoma, papillary thyroid carcinoma, and renal cell carcinoma.

Gene regulation has been widely used to predict potential imprinted genes with QPCT described as a maternally expressed imprinted gene [19]. This conclusion has been challenged by a report that QPCT is mistaken for an imprinted gene because of high expression in the decidual layer [20]. These latter data were obtained by embryo transfer to remove maternal contamination. However, embryo transfer experiments and in vitro fertilization might also influence imprinting status. While the function and role of glutaminyl peptide cyclase in human osteoporosis and in schizophrenia has been extensively studied, the function and role of glutathione-peptidyl-transferase has not been studied in crustaceans.

Experimental RNAi (RNA interference) in mammals is usually performed using siRNA (21–23 base pair duplexes) or shRNA (small hairpin RNA), as the introduction of long dsRNA to mammalian cells induces the interferon-based anti-viral response, resulting in cell death [21]. In contrast, long dsRNA does not adversely affect the cells of invertebrates, including worms, insects, and crustaceans, where it has been widely used to achieve efficient gene silencing. In the present study, we successfully developed a long-term RNAi method through multiple injections of long dsRNAs to *S. paramamosain*, in order to characterize the function of QPCT in viral and bacterial infection.

The coding sequence of QPCT consisted of 2445 nucleotides that contain an open reading frame of 370 amino acid residues. Phylogenetic analysis by neighbor-joining tree construction revealed a close evolutionary relationship between the QPCT's of *S. paramamosain* and *Trichinella spiralis*. QPCT is expressed at varying levels in all tissues that we evaluated in *S. paramamosain*, with highest levels in the intestines and with relatively low levels in the gills, hemolymph, gonad, hepatopancreas, heart, and muscle. High expression of QPCT in the intestine, a known immune organ in crustaceans, suggests that the expression of QPCT in different tissues might reflect various roles in the crab immune system. Intestinal has diverse microorganisms in mud crab, microorganisms produce and secrete a variety of enzymes, maintaining itself the microbial metabolism and helping absorb conversion and absorption of food and medicine. We infected healthy crabs with WSSV or with *V. alginolyticus* and thereafter examined the expression of QPCT by RT-qPCR. QPCT expression was significantly decreased upon infection with WSSV but was increased by *V. alginolyticus* infection. These results suggested that QPCT may play an important

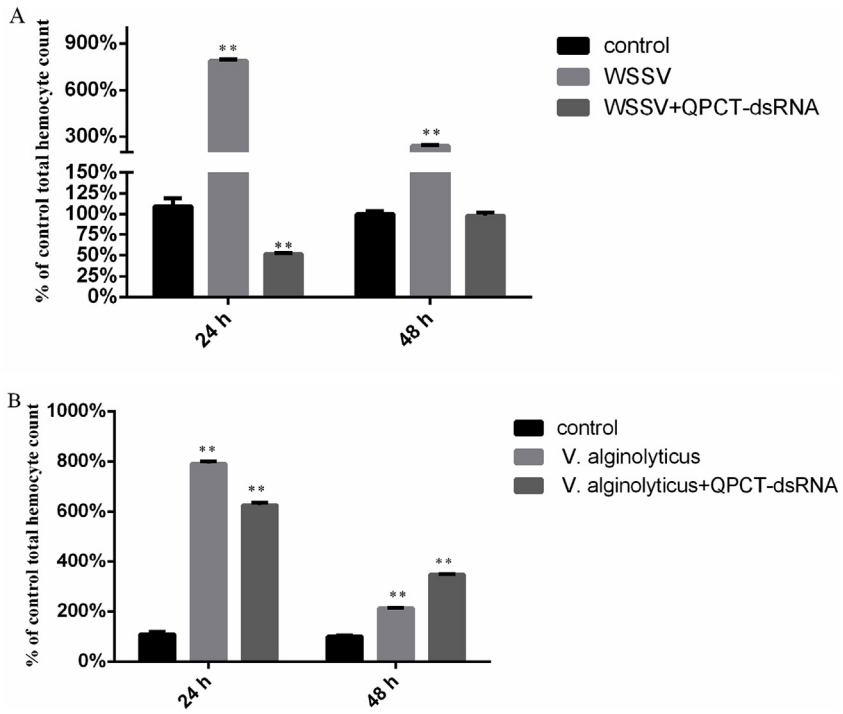

Fig. 10. The effect of QPCT knockdown on total hemocyte count. (A) THC of WSSV infected crabs pretreated with QPCT-dsRNA. (B) THC of *V. alginolyticus* infected crabs pretreated with QPCT-dsRNA. Data are expressed as percentage of the control. A double asterix indicates values significantly different ($P < 0.01$) from the control.

role in the innate immune system of the crab.

We then examined the role of QPCT in the innate immunity of *S. paramamosain,* by inhibiting its expression using QPCT-dsRNA. We also determined the effects of QPCT-dsRNA on the expression of several well-known innate immune proteins and signal transduction factors. Inhibition of QPCT expression resulted in significant down-regulation of the innate immune factors, prophenoloxidase (proPO) and crustin antimicrobial peptide, while myosin–essential-light-chain-like-protein was significantly up-regulated. These results suggested that QPCT affected the apoptotic and phagocytotic processes of crab hemocytes. Apoptosis is a highly regulated, programmed cell death process which plays a critical role in limiting virus infection [22]. In our study, apoptosis was decreased in WSSV infected crabs when pretreated with QPCT-dsRNA, indicating that QPCT may regulate apoptosis of host hemocytes and mediate apoptosis during WSSV infection.

The results of *V. alginolyticus* infection experiments indicated that QPCT may play a positive role in defending crabs against bacterial infection. However, lower replication of WSSV and decreased mortality in the QPCT knockdown group suggested that WSSV may utilize QPCT to promote its replication. We also found that fewer hemolymph cells were present in virus-infected crabs as compared with healthy crabs, with the opposite observed when crabs were infected with bacteria.

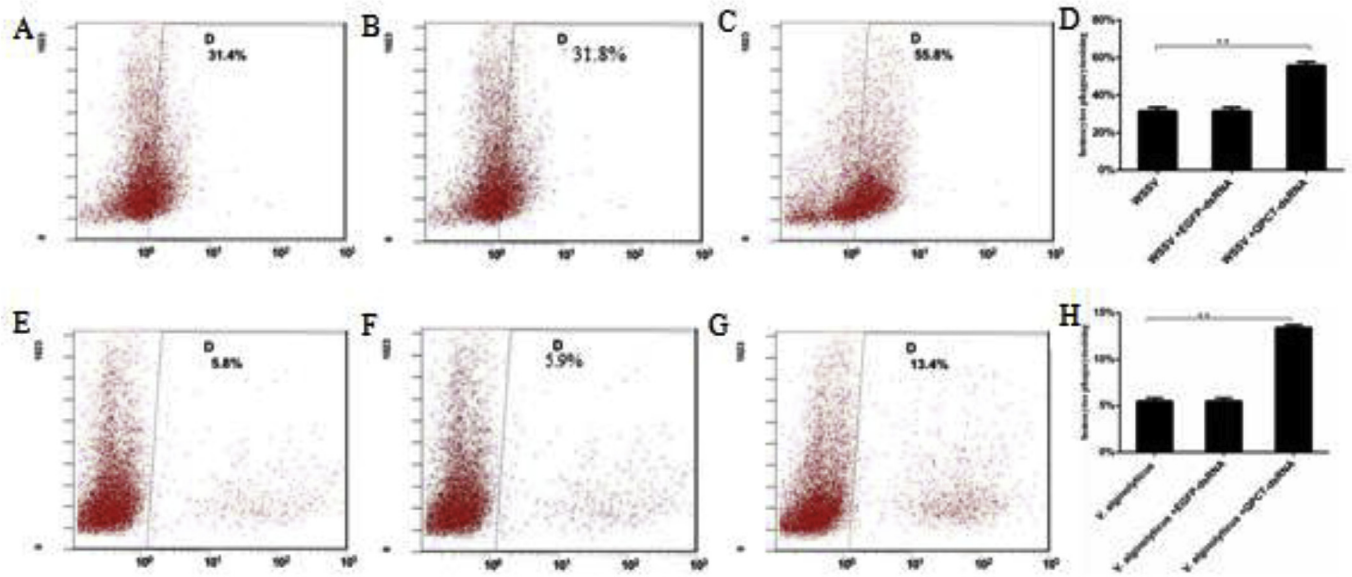

Fig. 11. Flow cytometric assay of phagocytosis. Inactivated WSSV virions and *V. alginolyticus* bacteria were labeled with FITC, incubated with hemocytes, and evaluated by flow cytometry. (A) WSSV infection control; (B) WSSV infection pretreated with EGFP-dsRNA; (C) WSSV infection pretreated with QPCT-dsRNA, (D) bar graph representation of WSSV cytometric results; (E) *V. alginolyticus* infection control; (F) *V. alginolyticus* infection pretreated with EGFP-dsRNA; (G) *V. alginolyticus* infection pretreated with QPCT-dsRNA; (H) bar graph representation of *V. alginolyticus* cytometric results. Double asterisks indicate a significant difference ($P < 0.01$) between the infection control and pre-treatment with dsRNA.

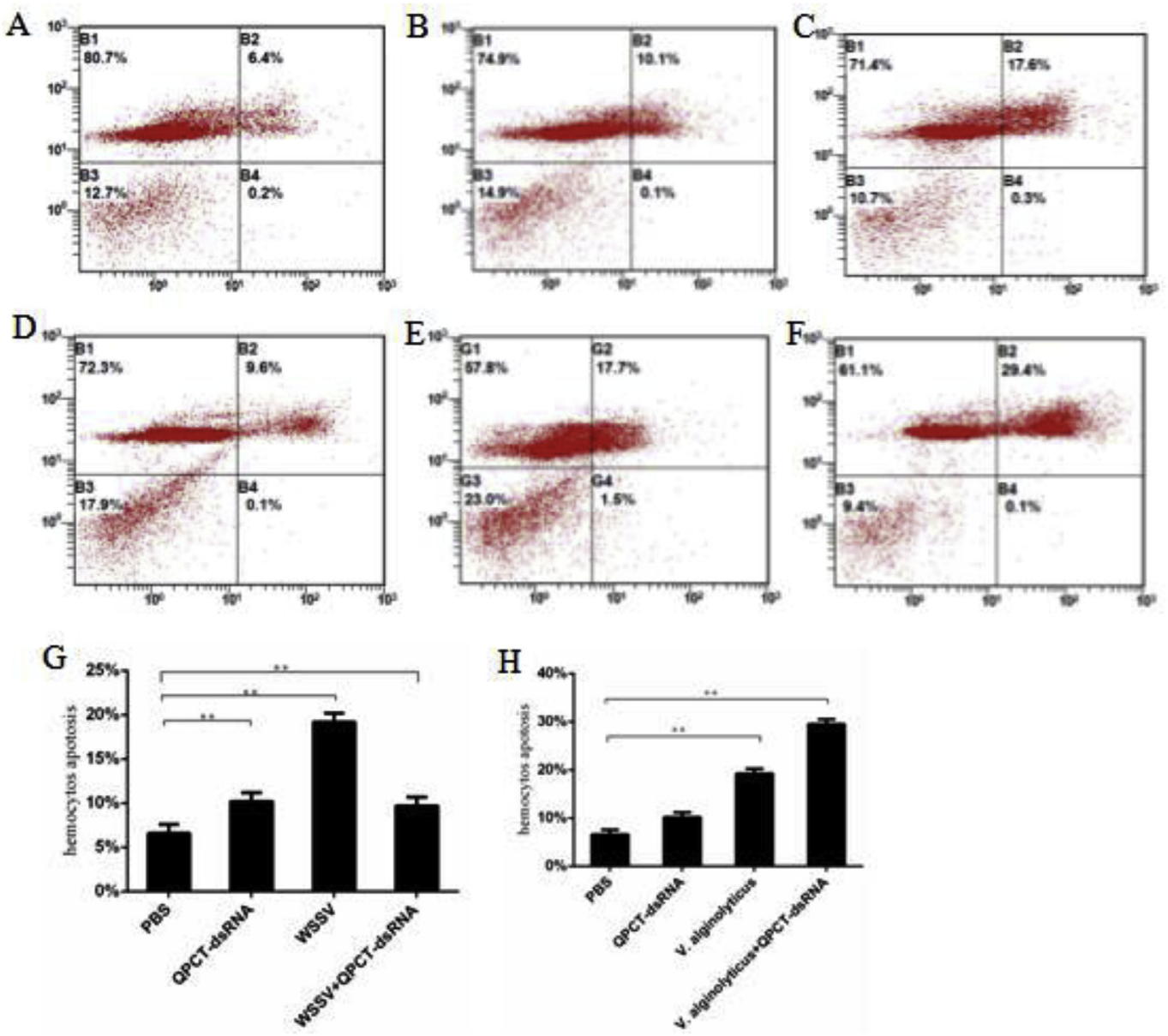

Fig. 12. Flow cytometry characterization of apoptosis in hemocytes. Animals were treated with (A) PBS; (B) QPCT-dsRNA; (C) infection with WSSV infection; (D) Infection with WSSV following pretreatment with QPCT-dsRNA; (E) *V. alginolyticus* infection; (F) Infection with *V. alginolyticus* following pretreatment with QPCT-dsRNA; (G) bar graph representation of phagocytosis results associated with WSSV; (H) bar graph representation of phagocytosis results associated with *V. alginolyticus*. Double asterisks indicate a significant difference ($P < 0.01$) between results, as indicated.

Furthermore, immune parameters such as proPO and SOD activities, as well as THC, were decreased upon reduction of QPCT.

This present study suggested that QPCT not only played a restrictive role in bacterial infection in crabs, but also influenced apoptosis and phagocytosis in hemocytes. QPCT therefore had an important immune activity in crabs. Our findings indicated that WSSV utilized the function of QPCT to inhibit host cell apoptosis, thereby promoting virion replication. The findings presented in this study provided an initial basis for further research into the function and role of glutathione-peptidyl-transferase in the innate immunity of invertebrates.

Acknowledgments

This work was financially supported by National Natural Science Foundation of China (31370050), and Qingjiang talent program (QJD1602023).

References

[1] C.A. Janeway Jr., R. Medzhitov, Innate immune recognition, Annu. Rev. Immunol. 20 (2002) 197–216.
[2] T. Zhang, L. Qiu, Z. Sun, et al., The specifically enhanced cellular immune responses in Pacific oyster (*Crassostrea gigas*) against secondary challenge with *Vibrio splendidus*, Dev. Comp. Immunol. 45 (2014) 141–150.
[3] J. Kurtz, Specific memory within innate immune systems, Trends Immunol. 26 (2005) 186–192.
[4] C.H. Wang, L. Chufang, L. Jiannhorng, et al., Purification and genomic analysis of baculovirus associated with white spot syndrome (WSSV) of *Penaeus monodon*, Dis Aquatic Organ 23 (1995) 239–242.
[5] S.B. Yuan, A.Y. Zhu, Progress on pathogenicity research on Vibrio alginolyticus to aquatic products, J. Zhejiang Ocean Univ. (Nat. Sci.) 3 (2012) 256–259.
[6] J.F. Zhou, W.H. Fang, L.L. Hu, et al., On proliferation of white spot syndrome virus (WSSV) within Green Mud Crab (*Scylla paramamosain*) by real time PCR, Marine Fisheries 34 (2012) 71–75.
[7] W.H. Busby, G.E. Quackenbush, J. Humm, et al., An enzyme(s) that converts glutaminyl-peptides into pyroglutamyl-peptides - presence in pituitary, brain, adrenal-medulla, and lymphocytes, J. Biol. Chem. 262 (1987) 8532–8536.
[8] G. Jing, H. Hongjuan, L. Qi, et al., Identification and epigenetic analysis of a

maternally imprinted gene qpct, Mol Cells 38 (2015) 859–865.
[9] F. Zhu, X. Zhang, Protection of shrimp against white spot syndrome virus (WSSV) with β-1,3-D-glucan-encapsulated vp28-siRNA particles, Mar. Biotechnol. 14 (2012) 63–68.
[10] M. Huang, Y. Liu, C. Xie, et al., LvDj-1, plays an important role in resistance against *Vibrio alginolyticus* in *Litopenaeus vannamei*, Fish Shellfish Immunol. 44 (2015) 180–186.
[11] K.J. Livak, T.D. Schmittgen, Analysis of relative gene expression data using real-time quantitative PCR and the 2(-delta delta c(t)) method, Methods 25 (2001) 402–408.
[12] F. Zhu, X. Zhang, The Wnt signaling pathway is involved in the regulation of phagocytosis of virus in *Drosophila*, Sci. Rep. 3 (2013) 2069.
[13] J. Zhihao, W. Lingling, J. Shuai, et al., Functional characterization of hemocytes from Chinese mitten crab *Eriocheir sinensis* by flow cytometry, Fish Shellfish Immunol. 69 (2017) 15–25.
[14] K. Wongprasert, T. Rudtanatip, J. Praiboon, Immunostimulatory activity of sulfated galactans isolated from the red seaweed *Gracilaria fisheri* and development of resistance against white spot syndrome virus (WSSV) in shrimp, Fish Shellfish Immunol. 36 (2014) 52–60.
[15] Z. Zhao, C. Jiang, X. Zhang, Effects of immunostimulants targeting Ran GTPase on phagocytosis against virus infection in shrimp, Fish Shellfish Immunol. 31 (2011) 1013–1018.
[16] C.O. Beauchamp, I. Fridovich, Isozymes of superoxide dismutase from wheat germ, Biochim. Biophys. Acta 317 (1973) 50–64.
[17] H.S. Jiang, D.Q. Dou, The miotransformation of arctin by human bacteria and enzymes, Mod. Chin. Med. 16 (2014) 9–11.
[18] M. Keyi, C. Jie, L. Zhiqiang, et al., Inhibitory effects of RNAi-mediated knockdown of EsDmrt-like gene on testicular development in the Chinese mitten crab *Eriocheir sinensis*, Aquaculture 463 (2016) 217–223.
[19] C.M. Brideau, K.E. Eilertson, J.A. Hagarman, et al., Successful computational prediction of novel imprinted genes from epigenomic features, Mol. Cell Biol. 30 (2010) 3357–3370.
[20] H. Okae, H. Hiura, Y. Nishida, et al., Re-investigation and RNA sequencing-based identification of genes with placenta-specific imprinted expression, Hum. Mol. Genet. 21 (2012) 548–558.
[21] D. Baltzis, S.Y. Li, A.E. Koromilas, Functional characterization of pkr gene products expressed in cells from mice with a targeted deletion of the N-terminus or C terminus domain of PKR, J. Biol. Chem. 277 (2002) 38364–38372.
[22] L.S. Young, C.W. Dawson, A.G. Eliopoulos, Viruses and apoptosis, Br. Med. Bull. 82 (1997) 65–76.